

# Poly lactide-cyclosporin A nanoparticles for targeted immunosuppression

Jamil Azzi,<sup>\*,†,1</sup> Li Tang,<sup>§,1</sup> Robert Moore,<sup>\*,‡</sup> Rong Tong,<sup>§</sup> Najib El Haddad,<sup>\*,‡</sup> Takurin Akiyoshi,<sup>\*,‡</sup> Bechara Mfarrej,<sup>\*,‡</sup> Sunmi Yang,<sup>\*,‡</sup> Mollie Jurewicz,<sup>\*,‡</sup> Takaharu Ichimura,<sup>\*,‡</sup> Neal Lindeman,<sup>†</sup> Jianjun Cheng,<sup>§,2</sup> and Reza Abdi<sup>\*,‡,2</sup>

<sup>\*</sup>Transplantation Research Center, Renal Division, and <sup>†</sup>Department of Pathology, Brigham and Women's Hospital and <sup>‡</sup>Children's Hospital Boston, Harvard Medical School, Boston, Massachusetts, USA, and <sup>§</sup>Department of Materials Science and Engineering, University of Illinois at Urbana-Champaign, Urbana, Illinois, US

**ABSTRACT** Polymeric nanoparticles (NPs), prepared *via* coprecipitation of drugs and polymers, are promising drug delivery vehicles for treating diseases with improved efficacy and reduced toxicity. Here, we report an unprecedented strategy for preparing poly lactide-cyclosporine A (PLA-CsA) NPs (termed CsA-NPs) through CsA-initiated ring-opening polymerization of lactide (LA) followed by nanoprecipitation. The resulting CsA-NPs have sub-100 nm sizes and narrow particle size distributions, and release CsA in a sustained manner without a “burst”-release effect. Both free CsA and CsA-NPs displayed comparable suppression of T-cell proliferation and production of inflammatory cytokines in various T-cell assays in a dose-dependent manner. The IC<sub>50</sub> values for CsA and CsA-NPs were 27.5 and 72.0 ng/ml, respectively. As lymph nodes are the main loci for T-cell activation, we coupled dendritic cells (DCs) with CsA-NPs and successfully delivered CsA selectively to the lymph nodes. Our studies indicated that CsA-NPs could be internalized in the DCs with a sustained release of CsA to the culture medium, suppressing alloreactive T-cell proliferation. Allogeneic DCs loaded with CsA-NPs were able to migrate to the draining lymph nodes where the T-cell priming was significantly reduced without any systemic release. This innovative nanoparticulate CsA delivery technology constitutes a strong basis for future targeted delivery of immunosuppressive drugs with improved efficiency and reduced toxicity.—Azzi, J., Tang, L., Tong, R., El Haddad, N., Akiyoshi, T., Mfarrej, B., Moore, R., Yang, S., Jurewicz, M., Ichimura, T., Lindeman, N., Cheng, J., Abdi, R. Poly lactide-cyclosporin A nanoparticles for targeted immunosuppression. *FASEB J.* 24, 3927–3938 (2010). [www.fasebj.org](http://www.fasebj.org)

**Key Words:** CsA toxicity • dendritic cells • targeted delivery

IMMUNOSUPPRESSIVE AGENTS HAVE played a pivotal role in ensuring the success of organ transplantation and have greatly improved the outcomes of patients with life-threatening, immune-mediated diseases (1). However, the use of immunosuppressive agents is

hindered by the lack of selectivity and frequently observed major adverse drug reactions. This problem is exemplified by cyclosporine A (CsA), the use of which results in a dramatic improvement in short-term allograft survival, although chronic CsA nephrotoxicity has been a major issue of chronic renal allograft loss due to its narrow therapeutic window (2–4). Targeted drug delivery systems can minimize undesired side effects of therapeutics by carrying the payload to the diseased tissues and directly releasing it there in a sustained manner (5). Among various drug delivery platforms being developed, polymeric nanoparticles (NPs), prepared by coprecipitating hydrophobic polymers and drugs, hold particular promise because of their ease of formulation and potential control of drug release through the degradation of polymers (6). NPs offer the possibility of incorporating multiple agents and protecting them from enzymatic degradation, thus enabling the systemic delivery and release of the therapeutic agents under spatio-temporal control (7). This new delivery modality has recently been reported for binding specifically to T cells (8) as a drug delivery vehicle and a noninvasive diagnostic tool for pathogenic T cells *in situ*, for codelivering immunosuppressant and chemotherapeutic agents, and for carrying antigens to induce potent cellular immunity for vaccination (8–10). However, current NPs typically have low drug loadings, uncontrolled encapsulation efficiencies, and significant drug burst-release effects when used *in vivo* (6, 11–13). These formulation challenges significantly limit their potential clinical applications. Here, we report the development of a novel strategy of preparing cyclosporine A-poly lactide

<sup>1</sup> These authors contributed equally to this work.

<sup>2</sup> Correspondence: R.A., Transplant Research Center, Brigham and Women's Hospital, 221 Longwood Ave, Boston, MA 02115, USA. E-mail: [rabdi@rics.bwh.harvard.edu](mailto:rabdi@rics.bwh.harvard.edu); J.C., Department of Materials Science and Engineering, University of Illinois at Urbana-Champaign, Urbana, IL 61801, USA. E-mail: [jianjunc@illinois.edu](mailto:jianjunc@illinois.edu)

doi: 10.1096/fj.10-154690

(CsA-PLA) conjugated nanoparticles through CsA/(BDI)ZnN(TMS)<sub>2</sub> [BDI, 2-((2,6-diisopropylphenyl)amido)-4-((2,6-diisopropylphenyl)imino)-2-pentene; TMS, trimethylsilyl] mediated ring-opening polymerizations of lactide (LA). This CsA-PLA conjugate was subsequently used for preparing CsA-PLA NPs (termed CsA-NPs in this article) *via* nanoprecipitation. This process is highly reproducible, can be easily scaled up, and results in NPs with superior physicochemical properties with excellent size control, narrow size distribution, and very well controlled release kinetics without burst-release effect. CsA-NPs showed excellent stability in biological media with negligible aggregation. Its capability for controlling the sustained release of CsA *in vitro* and suppressing T-cell mediated immune responses render CsA-NPs an excellent system for delivering immunosuppression for a wide variety of immune mediated disorders. We also developed a novel strategy combining CsA-NPs with dendritic cells (DCs) to efficiently deliver CsA to lymph nodes to inhibit T-cell priming without systemic release. This novel strategy can further improve the efficacy of the DC immune therapy used recently in various clinical trials as well as delivery of immunosuppressive drugs in general.

## MATERIALS AND METHODS

### Reagents

CsA was purchased from LC Laboratories (Woburn, MA, USA) and used as received. D,L-Lactide (LA) recrystallization, preparation of anhydrous solvents, NMR analysis of the drug-PLA conjugate, and HPLC analysis of the released drug ( $\lambda_{UV} = 207$  nm) were reported previously by us (14–15). (BDI)ZnN(TMS)<sub>2</sub>, the catalyst used for CsA-initiated LA polymerization, was prepared according to literature reported procedures (16) and used in our previous studies of controlled polymerization of cyclic esters (7, 14, 17–19). The sizes and polydispersities of NPs were determined on a ZetaPALS dynamic light scattering (DLS) detector (15 mW laser, incident beam=676 nm; Brookhaven Instruments, Holtsville, NY, USA). The lyophilization of NPs was completed on a benchtop lyophilizer (Freezone 2.5; Fisher Scientific, Pittsburgh, PA, USA).

### Synthesis and characterization of CsA-PLA polymer

In a glove box, (BDI)ZnN(TMS)<sub>2</sub> (17.8 mg, 0.029 mmol) and CsA (18.6 mg, 0.015 mmol) were mixed in anhydrous THF (0.5 ml) for 20 min. The recrystallized LA (54.0 mg, 0.375 mmol) in anhydrous THF (1.0 ml) was added dropwise to the mixture of CsA and (BDI)ZnN(TMS)<sub>2</sub>. The polymerization was monitored by checking the IR band of LA at 1771 cm<sup>-1</sup>. When the LA was completely consumed, the CsA-PLA was precipitated with ethyl ether (20 ml), washed with ethyl ether and methanol (20 ml) to remove BDI ligand, and dried to give the resulting CsA-PLA polymer. Any residual unreacted CsA was removed by washing the CsA-PLA with ethyl ether. The compositions of CsA-PLA were determined by <sup>1</sup>H-NMR. <sup>1</sup>H-NMR (CDCl<sub>3</sub>):  $\delta$  7.99 (d, 1 H), 7.63 (d, 1 H), 7.47 (d, 1 H), 7.18 (d, 1 H),

5.69 (dd, 1 H), 5.53 (broad, 1 H), 5.48 (d, 1 H), 5.23–5.12 (m, 113 H, CH of PLA), 4.82 (t, 1 H), 4.72 (d, 1 H), 4.64 (t, 1 H), 4.52 (t, 1 H), 4.35 (t, 1 H), 3.53 (s, 3 H), 3.39 (s, 3 H), 3.25 (s, 3 H), 3.10 (s, 3 H), 2.69 (s, 3 H), 2.68 (s, 3 H), and 1.59–1.53 (m, 339 H, CH<sub>3</sub> of PLA).

### Preparation of CsA-NPs and Cy5-containing CsA-NPs (CsA/Cy5-NPs)

A mixture of CsA-PLA (10 mg) and poly(lactide-*b*-methoxylated poly(ethylene glycol) (18) (PLA-mPEG,  $M_n = 19,400$  g/mol, 10 mg) in acetone (2 ml) was added dropwise to vigorously stirred nanopure water (40 ml). The NP suspension was then mixed for 6 h at room temperature to evaporate the organic solvent completely. CsA-NPs were collected by ultrafiltration using Amicon Ultra tubes (Ultracel membrane with 10<sup>5</sup> NMWL; Millipore, Billerica, MA, USA) at 3000 rpm for 15 min. Bovine serum albumin (BSA) was added as a lyoprotectant to the concentrated NP suspension at a BSA/NP mass ratio of 10:1. The mixture was lyophilized and stored at –20°C prior to use. The NPs were reconstituted with water and redispersed by brief sonication. The sizes and polydispersities of the resulting NPs were determined on a ZetaPALS DLS detector. To control the size of NPs, *N,N*-dimethylformamide (DMF) and tetrahydrofuran (THF) were also used as organic solvents to give smaller or larger particle sizes, respectively. NPs were prepared *via* nanoprecipitation as mentioned above at a CsA-PLA concentration of 1 to 10 mg/ml and an organic solvent to water volumetric ratio of 1:20. PLA conjugated with Cy5 (Cy5-PLA) was prepared by the procedure described previously (15). To prepare Cy5-containing CsA-NPs (CsA/Cy5-NPs), a mixture of CsA-PLA (5 mg), Cy5-PLA (5 mg) and PLA-mPEG ( $M_n = 19,400$  g/mol, 10 mg) in acetone (2 ml) was added dropwise to vigorously stirred nanopure water (40 ml). Subsequent steps were the same as those described for the CsA-NPs. Cy5-containing NPs without CsA (Cy5-NPs) were also prepared *via* nanoprecipitation and used as a control group.

### Determination of CsA-NP release kinetics

A PBS solution of CsA-NPs (0.43 mg/ml in 1× PBS) was prepared and placed in 6 separate tubes (8 ml) and incubated at 37°C. At the scheduled times (d 0, 4, 6, 8, 12, and 14), the NP solution was lyophilized. Ether (10 ml) was then added to extract released CsA. After the ether was evaporated, acetonitrile (500  $\mu$ l) was added. This solution was analyzed by HPLC to quantify the released CsA. The release kinetics was determined by quantifying the released CsA relative to the total CsA in CsA-NPs.

### Stability of CsA-NPs in salt solution

A DMF solution (100  $\mu$ l) of CsA-PLA (0.5 mg) and PLA-mPEG (0.5 mg) was added dropwise to vigorously stirred DI water (2 ml). Next, 10× PBS (233  $\mu$ l) was added to make the salt concentration equivalent to 1× PBS. The NP sizes were measured by DLS and followed for 40 min. Non-PEGylated NPs were prepared similarly without adding PLA-mPEG and used as control.

### Mixed lymphocyte reaction (MLR) and CD3/CD28 T-cell stimulation assays

MLR was performed as described previously (20). Briefly, in 96-well U-bottom plates, 5 × 10<sup>5</sup> each of responder and

irradiated stimulator splenocytes were cultured in triplicates in the presence of increasing dosages of free CsA, CsA-NPs (free CsA and CsA-NPs were added at the same equivalent dosage of CsA) and Cy5-NPs (Cy5-NPs were added at the same total NP concentration as CsA-NPs) for 48 h. Cultures were pulsed with 1  $\mu$ Ci of tritiated thymidine and the incorporation efficiencies were determined. Data are expressed as the mean  $\pm$  SD [ $^3$ H]-thymidine uptake (cpm) by triplicate cultures. For the CD3/CD28 stimulation assay, 100  $\mu$ l of anti-CD3 Ab diluted in PBS (1  $\mu$ g/ml, BD Biosciences, San Jose, CA) was added to each well of a 96-well flat bottom plate, placed at 37°C for 4 h, and then washed twice with PBS. Soluble anti-CD28 Ab (1  $\mu$ g/ml, BD Biosciences) was added to each well in the presence of  $5 \times 10^5$  responder splenocytes and an increasing concentration of free CsA, CsA-NPs and Cy5-NPs. Cultures were pulsed with tritiated thymidine as described above.

### Flow cytometry (FACS)

Splenocytes recovered from the recipients were resuspended in FACS buffer (PBS containing 1% FCS and 0.1% sodium azide). Cells were stained with rat anti-mouse CD8 PerCP, CD44 FITC, CD62l APC, CD69 FITC, CD80 FITC, CD86 PE, Annexin PE, 7 AAD PerCP, CD11c APC, and carboxyfluorescein succinimidyl ester (CFSE). All the antibodies were purchased from BD Biosciences and eBiosciences (San Diego, CA, USA). Flow cytometry was performed using a FACSCalibur (Becton Dickinson, Franklin Lakes, NJ, USA) and analyzed using CellQuest software (Becton Dickinson).

### ELISpot and luminex assays

The enzyme-linked immunosorbent spot (ELISpot) was performed as described previously by us (22). Briefly, ELISpot plates were coated with capture antibodies against interferon (IFN)- $\gamma$ . A total of  $5 \times 10^5$  splenocytes were cultured in triplicate in the presence of the same number of allogeneic splenocytes. Irradiated syngeneic splenocytes and Con A were used as negative and positive controls, respectively. Different concentrations of free CsA, CsA-NPs, and Cy5-NPs were added to the wells. After 48 h, the resulting spots were counted on a computer-assisted ELISpot image analyzer (Cellular Technology, Shaker Heights, OH, USA). To assess cytokine production of culture supernatant samples, a 21-plex cytokine kit (Millipore) was also used according to the manufacturer's instructions to analyze production of indicated cytokines.

### Internalization of CsA/Cy5-NPs by DCs and their delivery to T cells *in vitro*

To study the capability of DCs internalizing the CsA/Cy5-NPs, splenic DCs were purified from naive BALB/c mice using N418 magnetic beads and MidiMACS columns or AutoMACS (Miltenyi Biotec, Bergisch Gladbach, Germany) following the manufacturer's protocol. The DCs were then incubated in a CO<sub>2</sub> incubator for 3 h with CsA/Cy5-NPs (20,000 ng CsA equiv/ml) in a 24-well plate. The cells were then washed with  $1 \times$  PBS twice before being cytospinned, fixed on a slide, and stained with DAPI. To test the ability of the incubated DC with CsA/Cy5-NPs to potentially release CsA and suppress the proliferation of allogeneic T cells,  $3 \times 10^5$  BALB/c enriched CD4 T cells were incubated with three groups of  $2 \times 10^5$  C57Bl/6 DC treated with CsA/Cy5-NPs (20,000 ng CsA equiv/ml), medium, or an

equivalent dose of free CsA. Cultures were maintained for 3 d at 37°C in a humidified atmosphere of 5% CO<sub>2</sub> and then pulsed with 1  $\mu$ Ci of tritiated thymidine.

### Measurement of released CsA

Samples (50  $\mu$ l) were mixed with type I water (250  $\mu$ l), 0.1 mM zinc sulfate (250  $\mu$ l), and cyclosporin D (internal standard) in HPLC-grade methanol (500  $\mu$ l, 0.96  $\mu$ g/ml). The mixtures were vortexed for 30 s, incubated at room temperature for 5 min, and centrifuged for 5 min at 14,000 rpm. The supernatant (800  $\mu$ l) was transferred into vials for HPLC-MS/MS analysis. A reverse-phase column (TDM C18,  $2.1 \times 10$  mm; Waters Corp., Milford, MA) was used for the chromatographic separation of CsA. The supernatant (10  $\mu$ l) was analyzed by an Alliance 2795 HPLC (Waters) with a mobile phase of 1:1 methanol/water containing 2 mM ammonium acetate and 0.1% formic acid at a flow rate of 0.6 ml/min at 55°C. The HPLC fractions were eluted directly into and analyzed by an LC Quattro-Micro electrospray-tandem quadrupole mass spectrometer (Waters) for direct measurement of parent to daughter mass transitions for cyclosporin A (1219.9–1203.2  $m/z$ ) and cyclosporin D internal standard (1233.9–1217.0  $m/z$ ). The ratio of CsA/CsD was fit against a 6-point standard curve for quantification. The concentrations of CsA were reported in nanograms per milliliter and adjusted by subtracting the negative control values.

### CsA/Cy5-NPs pulsed DC trafficking to the draining lymph node *in vivo*

DCs ( $5 \times 10^6$ ) were incubated in a 24-well plate in a CO<sub>2</sub> incubator for 3 h with CsA/Cy5-NPs (20,000 ng CsA equiv/ml) and subsequently administered into both footpads of BALB/c mice ( $10^6$  DCs, 10  $\mu$ l PBS). The mice were euthanized 24 h after the administration of DCs. The popliteal lymph nodes were harvested and embedded in paraffin for histological analysis. Serial 6- $\mu$ m sections were collected *via* cryotome and transferred to glass microscope slides (3 sections/slide). To study the ability of the delivered NPs to suppress proliferation of T cells *in vivo*, we injected BALB/c mice footpads with 1 million allogeneic C57Bl/6 DCs incubated with CsA-NPs (20,000 ng CsA equiv/ml), medium, and free CsA. The popliteal lymph nodes were removed, teased into a single suspension in PBS, and stained for markers of cell activation as described below. The cells were assessed by a FACSCalibur (Becton Dickinson) for FACS analysis.

## RESULTS

### Synthesis of CsA-PLA polymer

To ensure a rapid and complete polymerization of LA at room temperature with CsA as the initiator, we utilized (BDI)ZnN(TMS)<sub>2</sub> as an active catalyst for the polymerization of LA (Fig. 1A) as previously reported by us (7, 14, 15). After the CsA was mixed with (BDI)ZnN(TMS)<sub>2</sub>, the (BDI)Zn-CsA complex, formed *in situ*, initiated and completed the polymerization of LA at room temperature within 12 h. The loading of CsA in CsA-PLA polymer was determined with <sup>1</sup>H-NMR by comparing the integrated peak area of the CH protons of PLA (5.12–5.23 ppm) with the NH proton

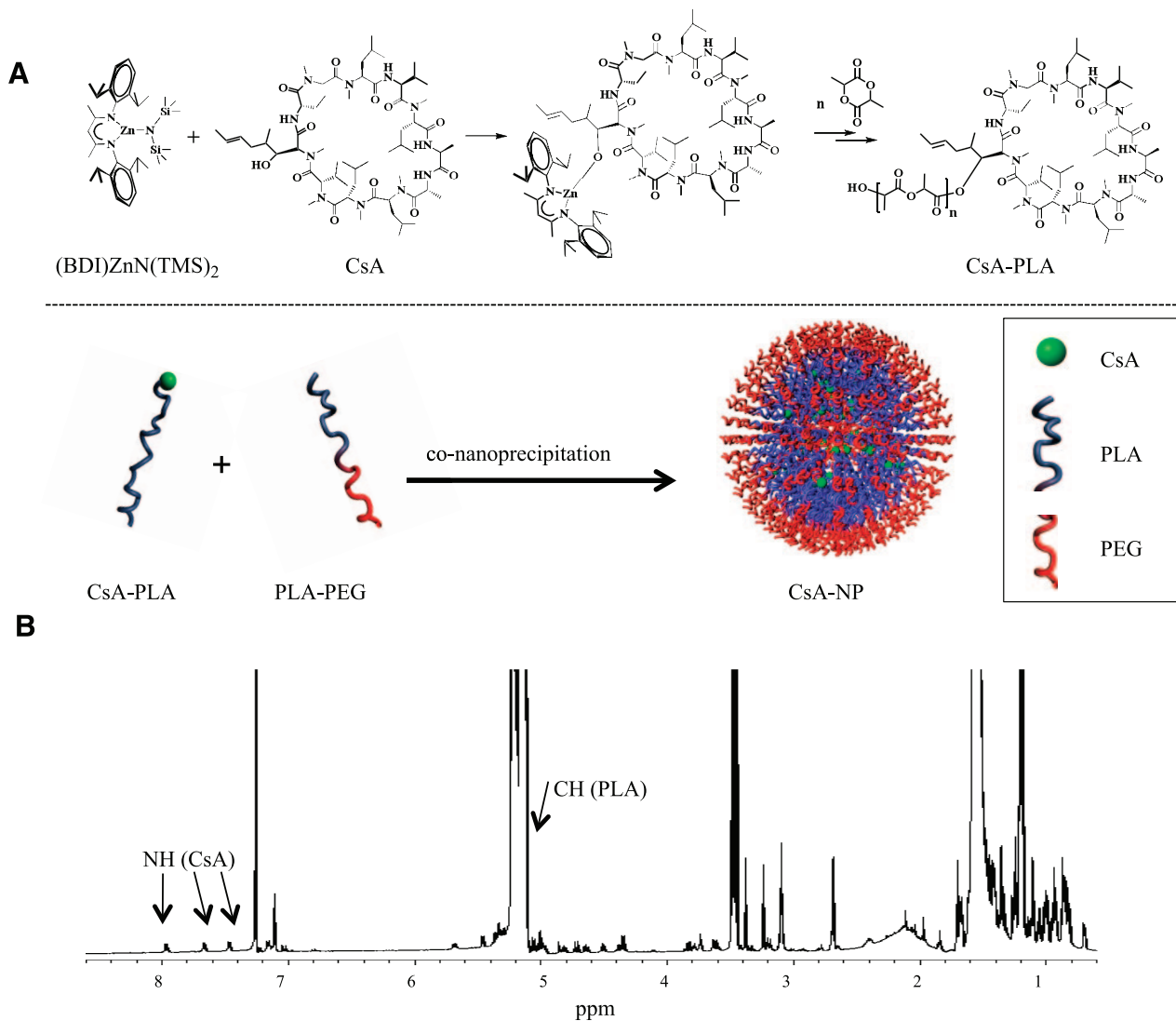


**Figure 1.** Preparation and characterization of CsA-NPs. *A*) Schematic illustration of preparation of PEG-coated CsA-PLA NPs by means of CsA-initiated LA polymerization in the presence of  $(\text{BDI})\text{ZnN}(\text{TMS})_2$ , followed by nanoprecipitation and noncovalent surface modification with poly(lactide-*b*-methoxyethylated PEG (PLA-mPEG). *B*) The loading of CsA in CsA-PLA polymer was calculated by comparing the integrated peak area of the CH protons of PLA (indicated by arrow) in the range of 5.12–5.23 ppm and the NH proton of CsA at 7.98, 7.63, and 7.47 ppm (indicated by arrow) and was found to be 7.1 wt%.

of CsA (7.98, 7.63, and 7.47 ppm) (Fig. 1*B*). The average CsA loading in CsA-PLA was found to be 7.1 wt%.

### Formulation of CsA-NPs via nanoprecipitation

Nanoprecipitation of CsA-PLA along with PLA-mPEG resulted in CsA-PLA/PLA-mPEG conjugated NPs (CsA-NPs) with a particle size of  $84.1 \pm 0.6$  nm and with nearly monomodal particle size distributions (Fig. 2*A*). The narrow, monomodal particle size distributions of the CsA-PLA/PLA-mPEG conjugated NPs were confirmed by the analysis of PLA NPs prepared with similar method by a scanning electronic microscope, as described in our previous studies (14), and are in sharp contrast to the multimodal particle size distribution typically observed with the NPs prepared by coprecipitation of a mix-

ture of free drug and hydrophobic polymer (6). As the multimodal distribution of NPs is due in part to the aggregation of the nonencapsulated drug molecules, the monomodal particle size distribution pattern observed and very low polydispersities with CsA-NPs are very likely related to the unimolecular structures of the CsA-PLA.

### Size control of CsA-NPs via nanoprecipitation

To control the NP sizes, we first studied the effect of the polymer concentration on NP size (6). When polymer concentrations were varied at a fixed solvent to water ratio, we observed a linear correlation of NP size with the polymer concentration (Fig. 2*B*). The NP size increased from 42.3 to 91.4 nm as the polymer concentration increased from 1 to 10 mg/ml in DMF. Similar trends were also observed

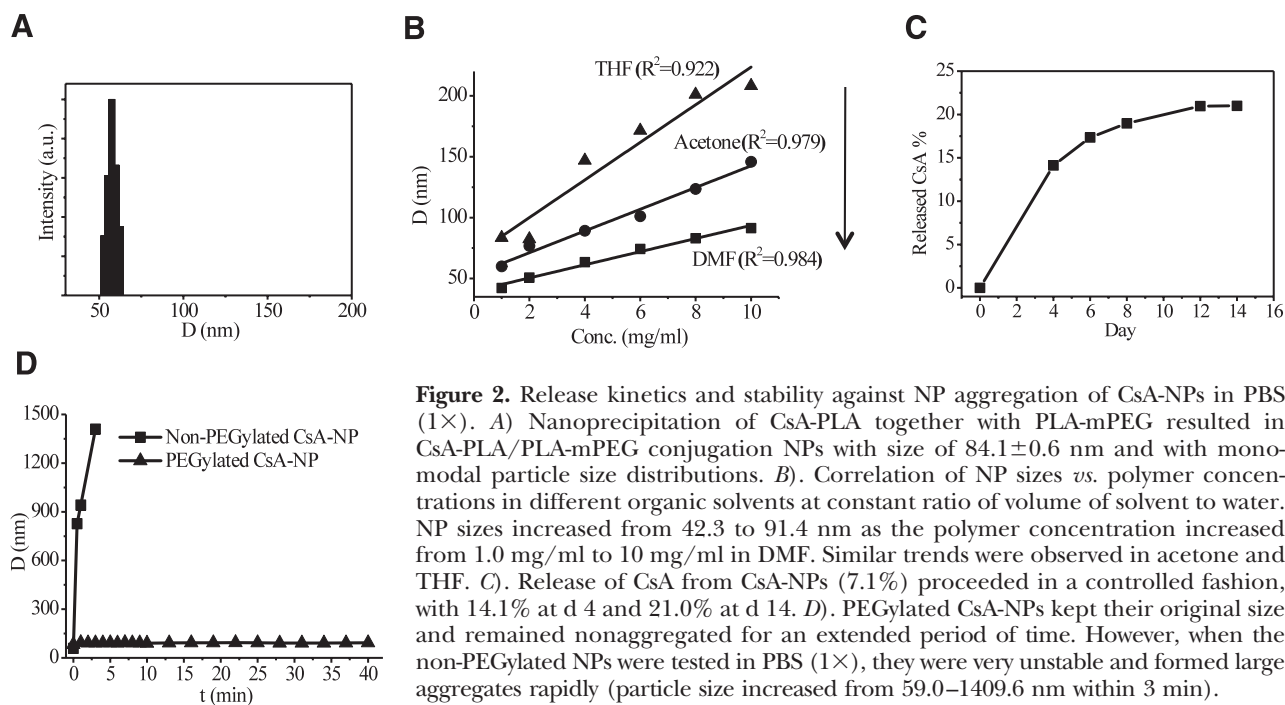


**Figure 2.** Release kinetics and stability against NP aggregation of CsA-NPs in PBS (1×). *A*) Nanoprecipitation of CsA-PLA together with PLA-mPEG resulted in CsA-PLA/PLA-mPEG conjugation NPs with size of  $84.1 \pm 0.6$  nm and with monomodal particle size distributions. *B*). Correlation of NP sizes *vs.* polymer concentrations in different organic solvents at constant ratio of volume of solvent to water. NP sizes increased from 42.3 to 91.4 nm as the polymer concentration increased from 1.0 mg/ml to 10 mg/ml in DMF. Similar trends were observed in acetone and THF. *C*). Release of CsA from CsA-NPs (7.1%) proceeded in a controlled fashion, with 14.1% at d 4 and 21.0% at d 14. *D*). PEGylated CsA-NPs kept their original size and remained nonaggregated for an extended period of time. However, when the non-PEGylated NPs were tested in PBS (1×), they were very unstable and formed large aggregates rapidly (particle size increased from 59.0–1409.6 nm within 3 min).

with acetone or THF as the solvent (Fig. 2*B*). As reported previously, the miscibility of the organic solvent also affects the size of NPs (6–7, 22). An increase in water miscibility leads to a decrease in the mean NP size when all other formulation parameters are held constant. We next investigated the effect of the type of organic solvent on the CsA-NP size. As expected, NPs prepared in DMF, the most water-miscible solvent tested, resulted in the smallest particles, which is presumably due to more efficient solvent diffusion and polymer dispersion into water (6). NPs prepared in acetone showed increased sizes (20–30 nm larger than those prepared in DMF). NPs prepared in THF, the least water-miscible solvents among solvents tested, had the largest particle size (Fig. 2*B*). Because acetone can be easily removed by evaporation, as compared to DMF, and the NPs prepared with this solvent have well-controlled, smaller sizes as compared the NPs prepared with THF as the solvent, we mainly used acetone as the solvent of PLA-CsA conjugate for the nanoprecipitation to prepare CsA-NPs (Fig. 2*B*).

#### Determination of the release kinetics of CsA-NPs

Drug burst release is a long-standing formulation challenge of drug-encapsulated NPs, which results in undesirable side effects and reduced therapeutic efficacy (13). Conventional drug-encapsulated NPs typically burst-release 60–90% of their payloads, because the release of the drug is controlled solely by diffusion (9). Since the CsA release kinetics from CsA-NPs is determined not only by diffusion but also by the hydrolysis of the CsA-PLA ester linker, the release of CsA from CsA-PLA conjugated NPs should

be more controllable with significantly reduced burst release (Fig. 2*C*). As expected, the release of CsA from CsA-NPs (7.1 wt%) proceeded in a controlled fashion, with 14.1% being released at d 4 with negligible burst-release effect.

#### Stability of CsA-NPs in salt solution

It is known that polymeric NPs tend to aggregate in biological conditions. To achieve prolonged systemic circulation and potential disease targeting, NPs should stay nonaggregated in physiological conditions. One approach is to modify NP surfaces PEGylation with poly(ethylene glycol) (PEG) (6, 23, 24). To reduce the efforts of removing unreacted reagents and by-products, we attempted to use a noncovalent approach to PEGylate NPs surface instead of covalently conjugating PEG to NPs (6, 25). We mixed CsA-PLA with PLA-PEG, an amphiphilic copolymer that has a 13-kDa PLA segment and a 5-kDa PEG, and used this mixture to prepare the PEGylated CsA-NPs. Significantly enhanced stability in PBS was observed; CsA-PLA/PLA-PEG NPs stayed nonaggregated for 40 min as compared to NPs without the PEG shell (Fig. 2*D*).

#### Capability of the CsA-NPs to suppress T-cell proliferation

To determine and compare the immunosuppressive abilities of CsA-NPs and free CsA in an *in vitro* model relevant to transplantation, various concentrations of CsA-NPs, free CsA, and Cy5-NPs were added to the MLR. MLR was performed using  $5 \times 10^5$  BALB/c responder and C57Bl/6 irradiated stimulator spleno-

cytes. We added free CsA and CsA-NPs at the equivalent dosage of CsA. Cy5-NPs were added at the same total NP concentration as CsA-NPs. Cy5-NPs containing no free CsA were used to assess any potential, undesired effect of NP materials on T cells. As compared to the positive control, free CsA delivered a dose-dependent inhibition of splenocytes proliferation in this assay (Fig. 3A). We found the same pattern of suppression by adding CsA-NPs (Fig. 3B). Equivalent concentrations of Cy5-NPs showed no suppression of T-cell proliferation (data not shown). In addition, the CD3-CD28 stimulation assay has traditionally been used to test the immunosuppressive effects of newly introduced drugs for various immune mediated diseases (26). Splenocytes ( $5 \times 10^5$ ) were stimulated with anti-CD3 and anti-CD28 Abs in triplicates in the presence of increasing dosage of free CsA, CsA-NPs, and Cy5-NPs for 2 d as described above. Similar to MLR, as compared to free CsA, our CsA-NPs efficiently suppressed T-cell proliferation in a dose-dependent manner (Fig. 3C, D, respectively).

### Ability of the CsA-NPs to suppress production of inflammatory cytokines in a similar fashion to free CsA

In addition to T-cell proliferation, it has been shown that the pattern of cytokines produced by activated T cells has an important role in the pathogenesis of T-cell-mediated diseases (27–29). We therefore tested the ability of our CsA-NPs to suppress the production of inflammatory cytokines. The fre-

quency of IFN- $\gamma$ -producing cells was first measured by ELISpot assay from cultured splenocytes of C57Bl/6 animals responding to BALB/c stimulating splenocytes *in vitro* (Fig. 4A–D). Measuring IFN- $\gamma$  by ELISpot has become a sensitive and common assay with highly reproducible results to examine alloreactive T-cell priming in the context of transplantation. All assays showed significant response to Con A (too numerous to count), indicating adequate viability of these cells. The number of spots in the wells with syngeneic splenocytes was used as the negative control. In all cases, the number of background spots was taken into consideration when analyzing the data. As compared to the positive control, the untreated stimulated cells, both free CsA and CsA-NPs comparably reduced the frequency of IFN- $\gamma$ -producing cells in a concentration-dependent manner starting at 10 ng/ml (Fig. 4A, B, respectively) ( $P < 0.05$ ). No suppression was observed with Cy5-NPs (Fig. 4C). Figure 4D represents the actual ELISpot plate at various conditions. The  $IC_{50}$  values for free CsA and CsA-NPs were calculated using the suppression of IFN- $\gamma$  producing cells in the ELISpot assay to be 27.5 ng/ml and 72.0 ng/ml, respectively (Fig. 4E). The higher  $IC_{50}$  of CsA-NPs is well correlated with the controlled, slow release property of CsA-NP. To evaluate the effect of the CsA-NPs on the production of inflammatory cytokines, which have increasingly been recognized for their role in the pathogenesis of autoimmunity and inflammatory diseases (27–29), we measured the production of IL-2, IL-4, IL-10, and IL-17 cytokines important in the regulation of T cells. Various concentrations of free CsA, CsA-NPs, and

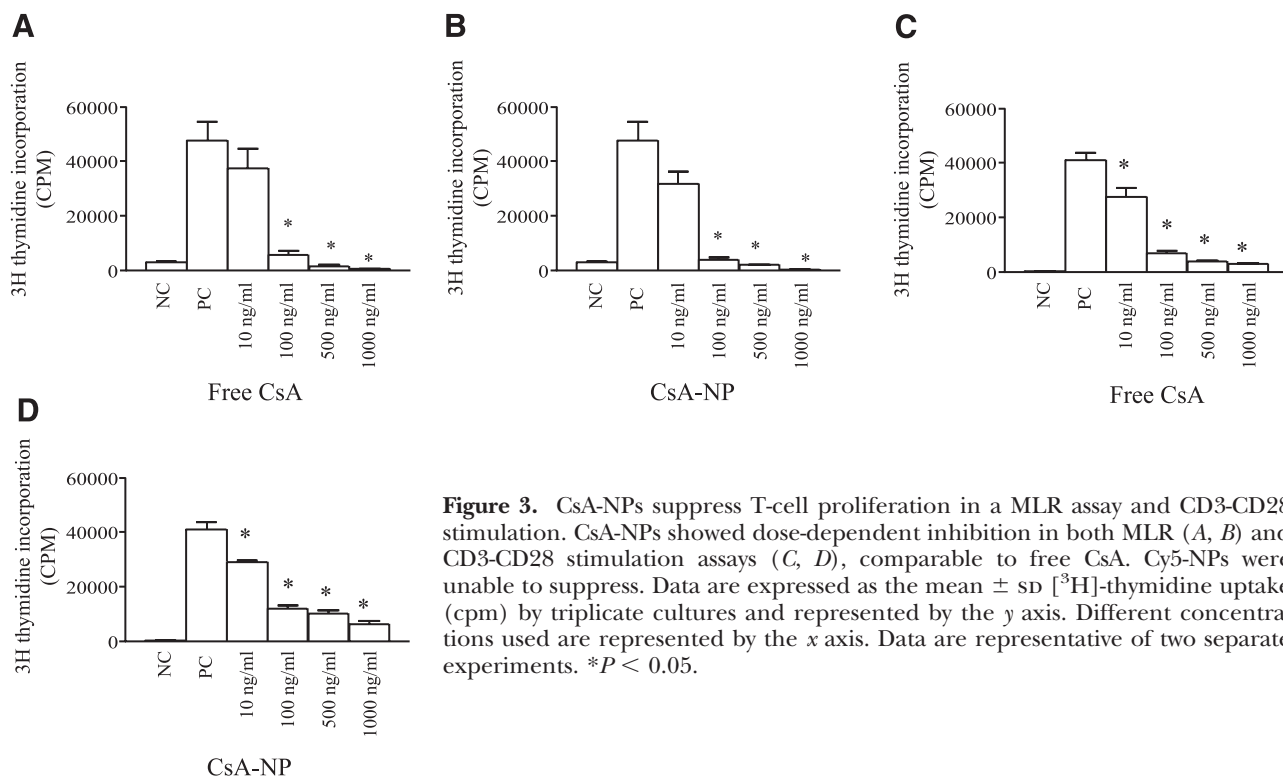


**Figure 3.** CsA-NPs suppress T-cell proliferation in a MLR assay and CD3-CD28 stimulation. CsA-NPs showed dose-dependent inhibition in both MLR (A, B) and CD3-CD28 stimulation assays (C, D), comparable to free CsA. Cy5-NPs were unable to suppress. Data are expressed as the mean  $\pm$  SD [ $^3$ H]-thymidine uptake (cpm) by triplicate cultures and represented by the y axis. Different concentrations used are represented by the x axis. Data are representative of two separate experiments. \* $P < 0.05$ .

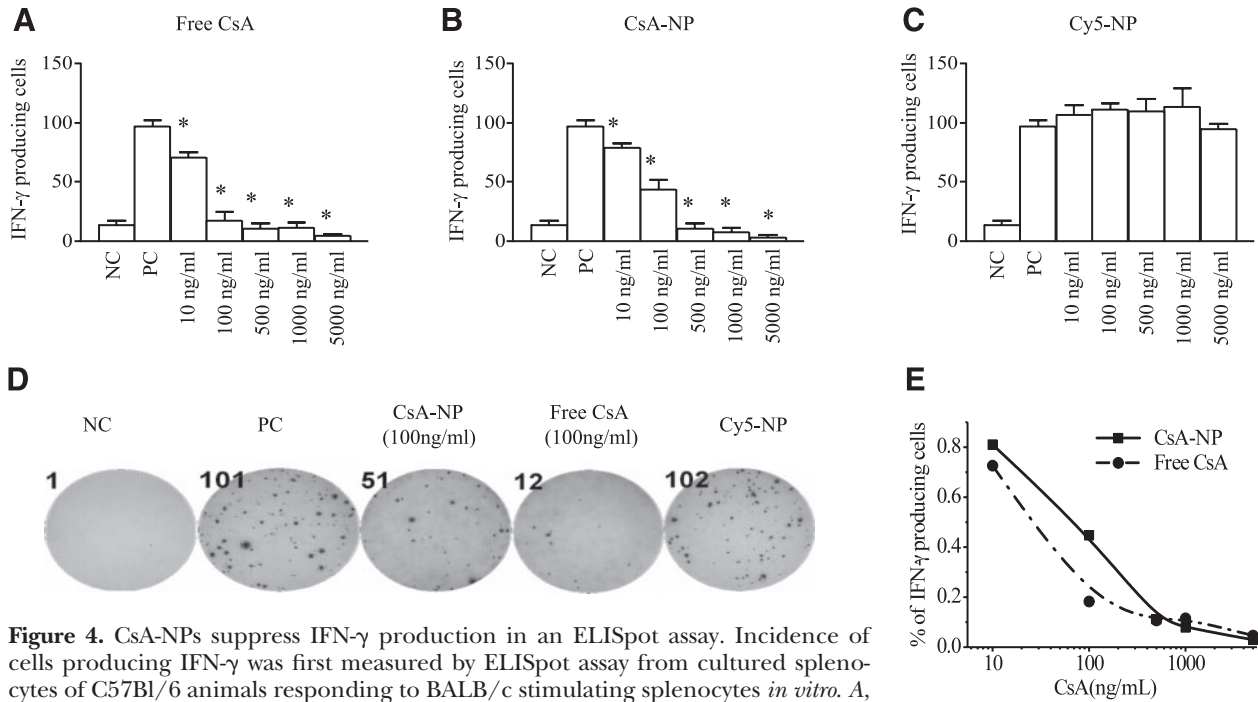


**Figure 4.** CsA-NPs suppress IFN- $\gamma$  production in an ELISpot assay. Incidence of cells producing IFN- $\gamma$  was first measured by ELISpot assay from cultured splenocytes of C57Bl/6 animals responding to BALB/c stimulating splenocytes *in vitro*. **A**, **B**) As compared to the positive control (untreated stimulated cells), both free CsA (**A**) and CsA-NPs (**B**) comparably reduced the frequency of IFN- $\gamma$ -producing cells in a concentration-dependent manner. **C**) No suppression was observed with Cy5-NPs. **D**) Representative wells of 100 ng/ml concentration of free CsA, CsA-NP, and Cy5-NP. **E**) IC<sub>50</sub> curves for free CsA and CsA-NP. Data are representative of 3 separate experiments. \* $P < 0.05$ .

Cy5-NPs were added to the MLR (described above), and the supernatant was collected to measure the level of aforementioned cytokines using a 21-plex cytokine kit (Millipore). Both free CsA and CsA-NPs comparably suppressed the production of these cytokines (**Fig. 5**). Cy5-NPs had no effect on cytokine production (data not shown).

#### Internalization of the CsA/Cy5-NPs by DC *in vitro* and their ability to suppress a MLR through release of CsA

To develop a strategy to efficiently deliver our NPs to the lymph nodes, we first examined whether the CsA-NPs could be effectively internalized by the

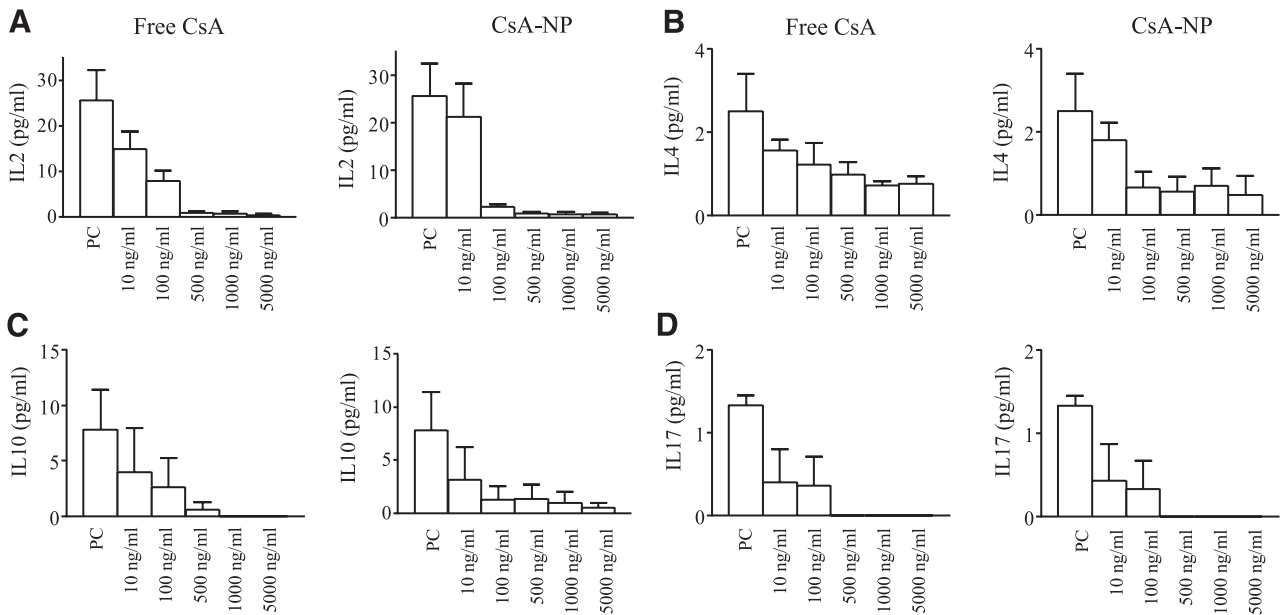


**Figure 5.** CsA-NPs suppress cytokine production in a similar fashion to free CsA. CsA-NPs (right panels) and free CsA (left panels) show the same pattern of suppression for the inflammatory cytokines measured: IL-2 (**A**), IL-4 (**B**), IL-10 (**C**), and IL-17 (**D**). Data are representative of 3 separate experiments in duplicate.

splenic DCs. Splenic DCs from BALB/c mice were MACS enriched, incubated in a CO<sub>2</sub> incubator at 37°C for 3 h with CsA/Cy5-NPs (20,000 ng CsA equiv/ml) in a 24-well plate. Cells were washed twice with PBS and then fixed on a slide. As shown in **Fig. 6A**, CsA/Cy5-NPs could be observed inside the DCs. To test the ability of our NPs loaded with DCs to deliver CsA to T cells *in vitro* and subsequently suppress T-cell proliferative responses when stimulated with CsA/Cy5-NPs pulsed allogeneic DCs and untreated DCs used as positive control. CD4 cells alone were used as a negative control. In addition, free CsA was used as another control. Thus, isolated DCs were treated with either CsA/Cy5-NPs, free CsA, or medium for 3 h and then washed twice with PBS to eliminate contamination. As shown in **Fig. 6B**, compared to CD4 T cells

alone, CD4 T cells efficiently proliferated when stimulated with untreated allogeneic DCs as positive control. When we stimulated CD4 T cells with CsA-NP-pulsed DCs (DC-CsA-NPs), we found that CD4 T-cell stimulation was significantly decreased as compared to untreated DCs ( $P=0.007$ ). However, virtually no proliferation was observed with DCs treated with free CsA (DC-free CsA) as compared to untreated DCs ( $P<0.0001$ ) (**Fig. 6B**).

To provide an explanation for the lack of proliferation using the DC-NP-CsA and DC-free CsA, we investigated whether NP-CsA and free CsA caused an increased DC death rate. We measured DC expression of apoptosis markers by FACS caliber in the three groups of cells. These include DCs treated with either 20,000 ng/ml free CsA, CsA/Cy5-NPs (at equivalent CsA dosage), or medium for 3 h. Cell

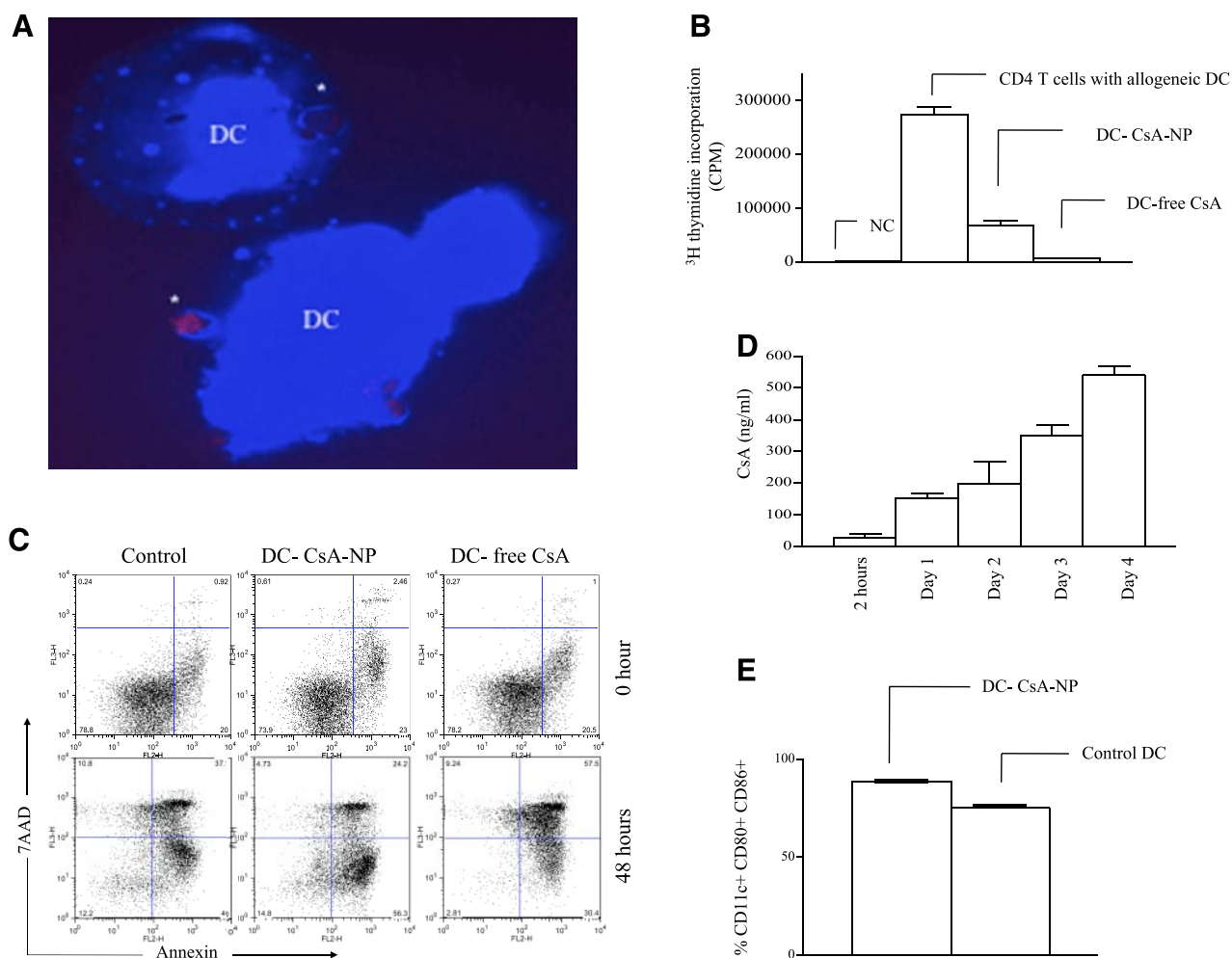


**Figure 6.** DCs uptake CsA/Cy5-NPs *in vitro* and suppress allogeneic T-cell proliferation in a MLR assay through release of free CsA. **A**) DCs incubated with CsA/Cy5-NPs were stained with DAPI (DNA stain, blue). Asterisk indicates two DCs engulfing Cy5-labeled particles. **B**) As compared to control or untreated CD4 cells, DC-CsA-NPs showed a significant decrease in stimulating CD4 T-cell proliferation ( $P=0.007$ ). DC-free CSA resulted in virtually no proliferation as compared to untreated DCs ( $P<0.0001$ ). Data are representative of 3 separate experiments. **C**) DCs treated with free CsA showed a >1-fold increase in cell death compared to cells treated with CsA/Cy5-NPs. Data are representative of 2 separate experiments. **D**) Supernatant was removed in triplicates at 2, 24, 48, 72, and 96 h to measure the release of CsA from DC-CsA-NPs; there was an increase in measured free CsA with respect to time. Data are representative of 2 separate experiments. **E**) As compared with untreated DCs, DCs treated with NP-CsA showed no significant change in the expression of maturity markers CD80 and CD86. Data are representative of 2 separate experiments.



death (positive for 7AAD and Annexin) and apoptosis (positive for Annexin and negative for 7AAD) were comparable in the three groups early on after 3 h of incubation (Fig. 6C). Those DCs, after 3 h of incubation, were then washed twice to eliminate contamination, cultured in a new medium for 48 h, and then apoptosis markers were checked again. The DCs treated with free CsA showed greater cell death compared to DCs treated with CsA/Cy5-NPs or medium ( $59.77 \pm 1.135$  vs.  $27.03 \pm 1.431$  vs.  $38.20 \pm 1.1\%$ , respectively, Fig. 6C). These results indicate that the DCs incubated with CsA containing NPs were not only protected from the toxicity of the CsA but were also able to suppress T-cell proliferation, through the sustained release of CsA over time. We therefore measured CsA release from the CsA/Cy5-NPs pulsed DCs over time. We incubated naive DCs with media containing 20,000 ng CsA equiv./ml CsA/Cy5-NPs for 3 h in a 24-well plate. DCs incubated with only medium were used as negative control. The DCs were then washed twice with PBS to eliminate contamination and were incubated in a CO<sub>2</sub> incubator at 37°C for 48 h in a 96-well plate. Supernatant was removed in triplicates at 2, 24, 48, 72, and 96 h. Figure 6D showed an increase in measured free CsA over time. Values of the negative controls were taken into consideration. We also assessed the effect of CsA-NPs and free CsA on DC maturation as a potential confounding reason contributing to the differential rate of proliferation of alloreactive T cells. DCs were incubated with either medium, CsA-NPs, or free CsA for 3 h. DC were then washed twice and cultured in a new medium for 16 h. The DC maturation (defined as CD80<sup>+</sup>CD86<sup>+</sup> cells by flow cytometry) showed a statistically insignificant increase in DC treated with CsA-NPs compared to untreated DC ( $88.35 \pm 0.2$  vs.  $75 \pm 0.5\%$ , respectively) (Fig. 6E).

#### Efficient trafficking of CsA/Cy5-NPs pulsed DC to the draining lymph nodes and suppression of T-cell proliferation *in vivo*

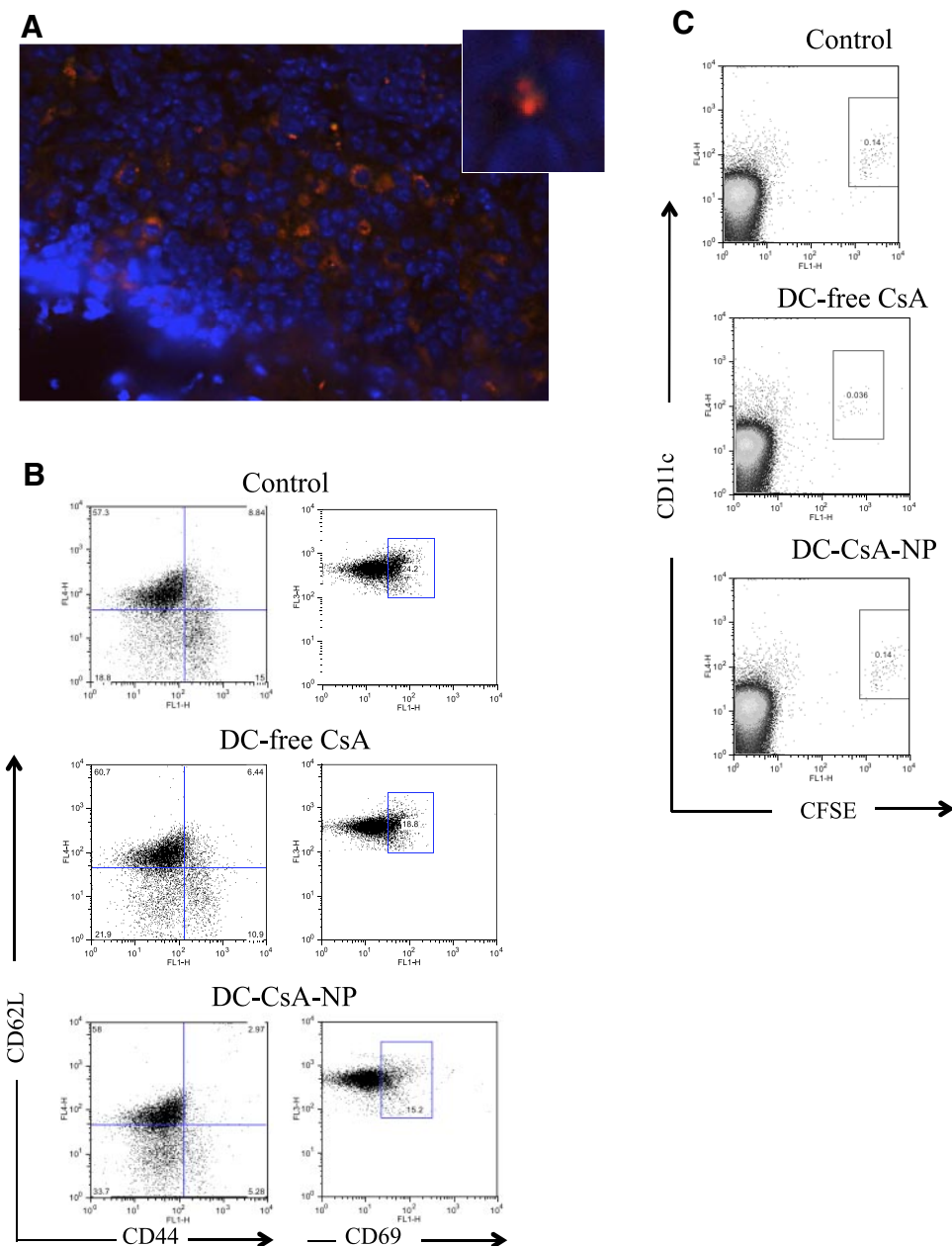
To examine the trafficking ability of our pulsed DCs to the draining lymph nodes, one million allogeneic C57Bl/6 DCs incubated with CsA/Cy5-NPs, suspended in 10 µl of PBS, were injected in the footpads of BALB/c mice. Mice were harvested 24 h later and popliteal lymph node embedded in paraffin. Figure 7A shows Cy5-stained cells in the popliteal lymph node, indicating successful delivery. Furthermore, we tested the ability of our delivered CsA-NPs to suppress T-cell stimulation at the level of the lymph node. We repeated the same experiment using DCs pulsed with CsA-NPs, free CsA, or medium as positive control. Popliteal lymph nodes were removed, teased into a single suspension in PBS and stained for markers of cell activation. CD8 effector T cells (CD44<sup>high</sup> CD62L<sup>low</sup>) were reduced in the group using DCs pulsed with CsA-NPs compared to mice treated with DCs incubated only with medium ( $6.3 \pm 1$

vs.  $14.8 \pm 1.4\%$ , respectively,  $P=0.002$ ; Fig. 7B, left panel). The expression of CD69 by CD8 T cells, as a marker of proliferation, was also significantly reduced in the group using DC pulsed with CsA-NPs compared to control as shown in Fig. 7B, right panel ( $15.3 \pm 0.9$  vs.  $22.2 \pm 1.7\%$ , respectively,  $P=0.019$ ). On the other hand, when DCs were incubated with free CsA, CD8 effector cells were slightly reduced compared to control ( $13.15 \pm 2$  vs.  $14.8 \pm 1.4\%$ , respectively,  $P=0.5$ ) as was CD69 expression of CD8 T cells ( $18.8 \pm 0.3$  vs.  $22.2 \pm 1.7\%$ , respectively,  $P=0.16$ ; Fig. 7B). We then examined whether this decrease in stimulation was due to differential migration of CsA- and CsA-NP-treated DCs to the lymph nodes. We repeated the same experiment with the CsA- and CsA-NP-pulsed DCs stained with CFSE. DCs incubated with medium or with NPs showed no difference in migration to lymph nodes at 24 h (Fig. 7C). The cells incubated with free CsA migrated less than the CsA-NP-treated cells ( $0.05 \pm 0.01$  vs.  $0.15 \pm 0.02\%$ , respectively,  $P=0.04$ ; Fig. 7C), most likely due to cell death as shown earlier (Fig. 6C). To check for systemic release of CsA, blood was drawn to measure CsA levels in mice injected with NP-CsA-loaded DCs or DCs treated with free CsA or medium at 2 and 24 h after injection. CsA measurements were comparable to negative control at both time points (data not shown).

## DISCUSSION

The past decade has witnessed major advancements in the development of new immunosuppressive drugs. The number of patients experiencing the toxicity associated with the use of these drugs, however, has also increased dramatically (1). Drug delivery techniques coupled with nanotechnology have provided therapeutic modalities for the treatment of a variety of diseases with improved efficacy and reduced side effects. Among various nanoparticle delivery systems being developed and evaluated, polymeric NPs represent one of the most promising and extensively investigated systems (12). Conventional polymeric NPs prepared *via* coprecipitation of polymers and drugs, however, have several formulation challenges remaining to be addressed (25). NPs typically have burst release of drugs when they are applied in aqueous solution. As much as 80–90% of the encapsulated drugs are burst released during the first few to tens of hours (19). The rapid dose dumping causes severe systemic toxicities (30). Unencapsulated drugs may self-aggregate (6) and can be very difficult to remove from the NPs, which challenges the processability and the clinical translation of NP delivery. An ideal solution to these problems is to covalently conjugate the drug molecules to the polymer through cleavable linkers, for instance ester linker. Formation of ester linker *via* conventional coupling chemistry (*e.g.*,

**Figure 7.** DCs deliver CsA/Cy5-NPs to the draining lymph nodes. DCs were incubated with CsA/Cy5-NPs and were injected in the footpad of a BALB/c mouse. Popliteal lymph nodes were harvested 48 h later and imaged with a Nikon 90I microscope. **A)** Cy5-stained cells in the popliteal lymph node. Inset: magnification of the lymph node image, representing a few cells and a Cy5-labeled compound. **B)** Popliteal lymph nodes were also teased into a single suspension in PBS and stained for markers of cell activation. As compared to the untreated DCs (control), percentages of CD8 effector T cells ( $CD44^{\text{high}} CD62L^{\text{low}}$ ) and  $CD8^+CD69^+$  were significantly lower using DC-CsA-NPs ( $14.8 \pm 1.4$  vs.  $6.3 \pm 1\%$ , respectively,  $P=0.002$ ). Although a lower percentage of effector cells was observed using the DC-free CsA, it did not reach statistical significance. **C)** DCs incubated with medium or with CsA-NPs showed comparable migration to lymph nodes at 24 h. Cells incubated with free CsA migrated significantly less than the CsA-NP-treated cells ( $0.05 \pm 0.01$  vs.  $0.15 \pm 0.02\%$ , respectively,  $P=0.04$ ). Data are representative of 3 separate experiments; 3–4 mice/group.



DCC/NHS coupling chemistry) can have extremely poor efficiency and require prolonged reaction. For molecules like CsA with complex structure, the steric bulk around its hydroxyl group will further complicate the ester bond formation. Here, we report the synthesis of CsA-PLA conjugate with CsA attached to PLA with an ester bond through CsA initiated ring-opening polymerization in the presence of  $(\text{BDI})\text{ZnN}(\text{TMS})_2$  (Fig. 1). The uncontrolled burst release of conventional polymeric NPs prepared *via* simple encapsulation was overcome by the preparation of CsA-PLA polymer conjugates through the LA polymerization mediated by  $\text{CsA}/(\text{BDI})\text{ZnN}(\text{TMS})_2$  with CsA being attached to PLA through a hydrolysable ester bond (Fig. 1). CsA-NPs with narrow size distribution and controlled release kinetics were readily achieved. By incorporating the favorable features of both conjugation and encapsulation in our design, our CsA-NPs were able to efficiently release CsA, which suppressed the proliferation and cyto-

kine production of activated T cells. Polymeric NPs prepared with encapsulating strategies in a hydrophobic polymer (*e.g.*, PLA) shielded the drug from the external environment, which limited its toxicity and allowed its coupling to cellular therapy. Because CsA-NPs were obtained through the entanglement of a large number of CsA-PLA conjugates, their sizes ( $\sim 100$  nm) were much larger than typical polymer-drug conjugates (2–5 nm). To compensate for the increase in NP size, which may limit its trafficking ability to lymph nodes, we coupled our NPs to DCs to create a new drug delivery strategy. DC immunotherapy has emerged over the recent years as a promising strategy to treat various diseases. There are several clinical trials that are currently underway in which DCs are being used as an adjuvant for vaccines, either as a direct therapy for type 1 diabetes (T1D) or to induce immunity against cancer (please refer to clinical trials.gov). In T1D, DCs were able to migrate to pancreatic lymph nodes when

injected subcutaneously in close proximity to the pancreas, which lead to the inhibition of T-cell interaction with pancreatic beta cells (31). Similarly, lymph nodes are a primary site where naive T cells meet antigen presenting cells, priming them into becoming alloreactive T cells (32). Lymph nodes therefore become attractive targets of systemically-administered, new immunotherapeutic modalities, such as NPs (8) or DCs, aiming for prolonged allograft survival (33) and efficient autoimmunity inhibition (31). While the trials mentioned above have created much excitement, we are proposing a novel strategy to further improve the efficacy of the DCs for immunotherapy by loading them with NPs that can carry different classes of drugs, such as CsA. We hypothesized that DCs would phagocytose the NPs and readily migrate to the draining lymph nodes since our conjugated nanoparticle technique on CsA would protect the DCs from cell death. We demonstrated that the CsA-NPs internalized by DCs *in vitro* were able to release CsA to the culture medium (Fig. 6D) and suppress T-cell proliferation. This observation cannot be ascribed to DC death, as our apoptosis studies showed that there was no significant difference of apoptosis for cells treated with medium or CsA-NPs. In contrast, DCs treated with free CsA showed significantly reduced viability at 48 h compared to the control and NP-treated cells. Thus, CsA-NPs provided protection for the carrier cells from the toxicity of the medication, thus allowing the cells to migrate to the target organ. In addition, DCs coupled with CsA-NPs did not show decreased maturation, which could have explained some of the observed suppression of T cells. We then tested whether pulsed DCs with CsA/Cy5-NPs were able to traffic to lymph nodes. Our data using the injection of pulsed DCs into footpads showed efficient trafficking of DC to the draining lymph nodes. Interestingly, compared to trafficked allogeneic DCs, which naturally give rise to a robust generation of alloreactive T cells (control DCs), CsA/Cy5-NPs loaded DCs efficiently suppressed proliferation and activation of CD8 T cells in the lymph node without any systemic release of CsA. In summary, we report the development of a novel CsA-PLA conjugated NP delivery system for targeted immunosuppression. The CsA-NPs that stay nonaggregated in physiological media were able to release CsA in a sustained manner *in vitro* and suppress the T-cell-mediated immune response through the released CsA. Coupling CsA-NPs with allogeneic DCs allowed for increased delivery of drugs to the lymph nodes which facilitated efficient inhibition of T-cell priming in draining lymph nodes in a locally controlled and sustained manner with no systemic release. Our study demonstrated that employing nanotechnology in immunosuppression may not only provide a far more efficient way to inhibit autoreactive or alloreactive T cells but also minimize undesirable organ toxicity. **[F]**

The authors thank Elizabeth Glidden for her assistance in measuring CsA. This work was supported by a National Kidney Foundation clinical scientist award, a Roche Organ Transplantation Research Foundation grant, a Juvenile Diabetes Research Foundation regular grant, a John Merrill Transplant Scholar grant (to R.A.), National Science Foun-

dation Career Program grant DMR-0748834 (to J.C.), U.S. National Institutes of Health grants 1R21CA139329-01 and 1R21EB009486-01 (to J.C.), the Siteman Center for Cancer Nanotechnology Excellence (SCCNE; Washington University, St. Louis, MO, USA), the Center for Nanoscale Science and Technology (CNST; University of Illinois at Urbana-Champaign; to J.C.), and a Prostate Cancer Foundation Competitive Award Program grant (to J.C.).

## REFERENCES

1. Kaplan, B., and Meier-Kriesche, H. U. (2004) Renal transplantation: a half century of success and the long road ahead. *J. Am. Soc. Nephrol.* **15**, 3270–3271
2. Wong, W., Venetz, J. P., Tolkoff-Rubin, N., and Pascual, M. (2005) Immunosuppressive strategies in kidney transplantation: which role for the calcineurin inhibitors? *Transplantation* **80**, 289–296
3. Chapman, J. R., and Nankivell, B. J. (2006) Nephrotoxicity of ciclosporin A: short-term gain, long-term pain? *Nephrol. Dial. Transpl.* **21**, 2060–2063
4. Neto, A. B., Haapalainen, E., Ferreira, R., Feo, C. F., Misiako, E. P., Vennarecci, G., Porcu, A., Dib, S. A., Goldenberg, S., Gomes, P. O., and Nigro, A. T. (1999) Metabolic and ultrastructural effects of cyclosporin A on pancreatic islets. *Transpl. Int.* **12**, 208–212
5. Alvarez-Lorenzo, C., and Concheiro, A. (2008) Intelligent drug delivery systems: polymeric micelles and hydrogels. *Mini. Rev. Med. Chem.* **8**, 1065–1074
6. Cheng, J., Teply, B. A., Sherifi, I., Sung, J., Luther, G., Gu, F. X., Levy-Nissenbaum, E., Radovic-Moreno, A. F., Langer, R., and Farokhzad, O. C. (2007) Formulation of functionalized PLGA-PEG nanoparticles for *in vivo* targeted drug delivery. *Biomaterials* **28**, 869–876
7. Tong, R., and Cheng, J. (2010) Controlled synthesis of camptothecin-poly(lactide) conjugates and nanoconjugates. *Bioconjug. Chem.* **21**, 111–121
8. Fahmy, T. M., Schneck, J. P., and Saltzman, W. M. (2007) A nanoscopic multivalent antigen-presenting carrier for sensitive detection and drug delivery to T cells. *Nanomedicine* **3**, 75–85
9. Musumeci, T., Ventura, C. A., Giannone, I., Ruozi, B., Montenegro, L., Pignatello, R., and Puglisi, G. (2006) PLA/PLGA nanoparticles for sustained release of docetaxel. *Int. J. Pharmaceutics* **325**, 172–179
10. Wang, X., Uto, T., Akagi, T., Akashi, M., and Baba, M. (2007) Induction of potent CD8+ T-cell responses by novel biodegradable nanoparticles carrying human immunodeficiency virus type 1 gp120. *J. Virol.* **81**, 10009–10016
11. Panyam, J., and Labhasetwar, V. (2003) Biodegradable nanoparticles for drug and gene delivery to cells and tissue. *Adv. Drug Deliv. Rev.* **55**, 329–347
12. Tong, R., and Cheng, J. J. (2007) Anticancer polymeric nanomedicines. *Polymer. Rev.* **47**, 345–381
13. Soppimath, K. S., Aminabhavi, T. M., Kulkarni, A. R., and Rudzinski, W. E. (2001) Biodegradable polymeric nanoparticles as drug delivery devices. *J. Control. Release* **70**, 1–20
14. Tong, R., and Cheng, J. (2008) Paclitaxel-initiated, controlled polymerization of lactide for the formulation of polymeric nanoparticulate delivery vehicles. *Angew. Chem. Int. Ed. Engl.* **47**, 4830–4834
15. Chaney, E. J., Tang, L., Tong, R., Cheng, J., and Boppart, S. (2010) Lymphatic biodistribution of polylactide nanoparticles. *Mol. Imaging* **9**, 153–162
16. Chamberlain, B. M., Cheng, M., Moore, D. R., Ovitt, T. M., Lobkovsky, E. B., and Coates, G. W. (2001) Polymerization of lactide with zinc and magnesium beta-diiminate complexes: stereocontrol and mechanism. *J. Am. Chem. Soc.* **123**, 3229–3238
17. Tong, R., and Cheng, J. J. (2009) Ring-opening polymerization-mediated controlled formulation of polylactide-drug nanoparticles. *J. Am. Chem. Soc.* **131**, 4744–4754
18. Tong, R., Yala, L., Fan, T. M., and Cheng, J. (2010) Aptamer-coated paclitaxel-poly(lactide) nanoconjugates: formulation and cancer targeting. *Biomaterials* **31**, 3043–3053

19. Tong, R., Christian, D. A., Tang, L., Cabral, H., Baker, J. R., Kataoka, K., Discher, D. E., and Cheng, J. J. (2009) Nanopolymeric therapeutics. *MRS Bulletin* **34**, 422–431
20. Izawa, A., Ueno, T., Jurewicz, M., Ito, T., Tanaka, K., Takahashi, M., Ikeda, U., Sobolev, O., Fiorina, P., Smith, R. N., Hynes, R. O., and Abdi, R. (2007) Importance of donor- and recipient-derived selectins in cardiac allograft rejection. *J. Am. Soc. Nephrol.* **18**, 2929–2936
21. Fiorina, P., Jurewicz, M., Vergani, A., Augello, A., Paez, J., Ricchiuti, V., Tchepachvili, V., Sayegh, M. H., and Abdi, R. (2008) Phenotypic and functional differences between wild-type and CCR2<sup>-/-</sup> dendritic cells: implications for islet transplantation. *Transplantation* **85**, 1030–1038
22. Galindo-Rodriguez, S., Allemann, E., Fessi, H., and Doelker, E. (2004) Physicochemical parameters associated with nanoparticle formation in the salting-out, emulsification-diffusion, and nanoprecipitation methods. *Pharm. Res.* **21**, 1428–1439
23. Caliceti, P., and Veronese, F. M. (2003) Pharmacokinetic and biodistribution properties of poly(ethylene glycol)-protein conjugates. *Adv. Drug Deliv. Rev.* **55**, 1261–1277
24. Farokhzad, O. C., Cheng, J., Teply, B. A., Sherifi, I., Jon, S., Kantoff, P. W., Richie, J. P., and Langer, R. (2006) Targeted nanoparticle-aptamer bioconjugates for cancer chemotherapy in vivo. *Proc. Natl. Acad. Sci. U. S. A.* **103**, 6315–6320
25. Gref, R., Minamitake, Y., Peracchia, M. T., Trubetskoy, V., Torchilin, V., and Langer, R. (1994) Biodegradable long-circulating polymeric nanospheres. *Science* **263**, 1600–1603
26. Sakuma, S., Kato, Y., Nishigaki, F., Magari, K., Miyata, S., Ohkubo, Y., and Goto, T. (2001) Effects of FK506 and other immunosuppressive anti-rheumatic agents on T cell activation mediated IL-6 and IgM production in vitro. *Int. Immunopharmacol.* **1**, 749–757
27. Abdi, R., Smith, R. N., Makhoulouf, L., Najafian, N., Luster, A. D., Auchincloss, H., Jr., and Sayegh, M. H. (2002) The role of CC chemokine receptor 5 (CCR5) in islet allograft rejection. *Diabetes* **51**, 2489–2495
28. Yuan, X., Paez-Cortez, J., Schmitt-Knosalla, I., D'Addio, F., Mfarrej, B., Donnarumma, M., Habicht, A., Clarkson, M. R., Iacomini, J., Glimcher, L. H., Sayegh, M. H., and Ansari, M. J. (2008) A novel role of CD4 Th17 cells in mediating cardiac allograft rejection and vasculopathy. *J. Exp. Med.* **205**, 3133–3144
29. Lohr, J., Knoechel, B., Wang, J. J., Villarino, A. V., and Abbas, A. K. (2006) Role of IL-17 and regulatory T lymphocytes in a systemic autoimmune disease. *J. Exp. Med.* **203**, 2785–2791
30. Matsumura, Y., Hamaguchi, T., Ura, T., Muro, K., Yamada, Y., Shimada, Y., Shirao, K., Okusaka, T., Ueno, H., Ikeda, M., and Watanabe, N. (2004) Phase I clinical trial and pharmacokinetic evaluation of NK911, a micelle-encapsulated doxorubicin. *Br. J. Cancer* **91**, 1775–1781
31. Giannoukakis, N., Phillips, B., and Trucco, M. (2008) Toward a cure for type 1 diabetes mellitus: diabetes-suppressive dendritic cells and beyond. *Pediatr. Diabetes* **9**, 4–13
32. Mempel, T. R., Henrickson, S. E., and Von Andrian, U. H. (2004) T-cell priming by dendritic cells in lymph nodes occurs in three distinct phases. *Nature* **427**, 154–159
33. Xu, M. Q., Suo, Y. P., Gong, J. P., Zhang, M. M., and Yan, L. N. (2004) Prolongation of liver allograft survival by dendritic cells modified with NF-kappaB decoy oligodeoxynucleotides. *World J. Gastroenterol.* **10**, 2361–2368

*Received for publication January 25, 2010.*

*Accepted for publication May 27, 2010.*